

## Modelling and Mapping Electrical Resistance Changes Due to Hearth Erosion in a 'Cold' Model of a Blast Furnace

M. Wang<sup>#</sup>, S. Johnstone<sup>\*</sup>, W.J.N. Pritchard<sup>\*</sup> and T.A. York<sup>#</sup>,

<sup>#</sup>Department of Electrical Engineering and Electronics  
UMIST. P.O. Box 88, Manchester M60 1QD, UK

<sup>\*</sup>Teesside Technology Centre, British Steel  
P.O. Box 11 Grangetown, Middlesbrough Cleveland TS6 6UB  
Tel: +44 161 200 4786, Fax: +44 161 2004789, Email: mi.wang@umist.ac.uk

*MW and TY are members of the Virtual Centre for Industrial Process Tomography*

**Abstract** - A study of the use of electrical resistance tomography for imaging hearth wall thickness is reported. A significant challenge is to acquire accurate measurements of the very low resistivity in the hearth which is constructed with graphite bricks (conductivity =  $2.5 \cdot 10^4$  S/m). A noise model of the blast furnace for electrical measurements, an experimental 'cold' furnace model (0.5 m in diameter) and a 3-D simulation model are established. Results from these models are described.

**Keywords** : Electrical resistance tomography, Hearth erosion, Carbon, Sensitivity theorem.

### 1. INTRODUCTION

The life of a furnace is essentially limited by the wear of the hearth. It is necessary to measure and monitor the hearth wall thickness during the operational 'campaign' in order to be able to predict when the furnace requires relining. Erosion is usually monitored with thermal sensors embedded inside the hearth [1]. In recent years ultrasonic techniques have also been adopted for the purpose [2]. This paper describes a study of the use of electrical resistance tomography for imaging hearth wall thickness. A significant challenge is to acquire accurate measurements of the very low resistivity in the hearth which is constructed with graphite bricks (conductivity =  $2.5 \cdot 10^4$  S/m) [3].

Three models are established for the study. They are a noise model for analyzing and searching optimum methods to obtain accurate electrical measurements from the blast furnace, a 3-D simulation model for validating and simulating boundary conditions from physical setups, and an experimental 'cold' model (0.5 m in diameter) for acquiring data physically. Results obtained from these models are reported.

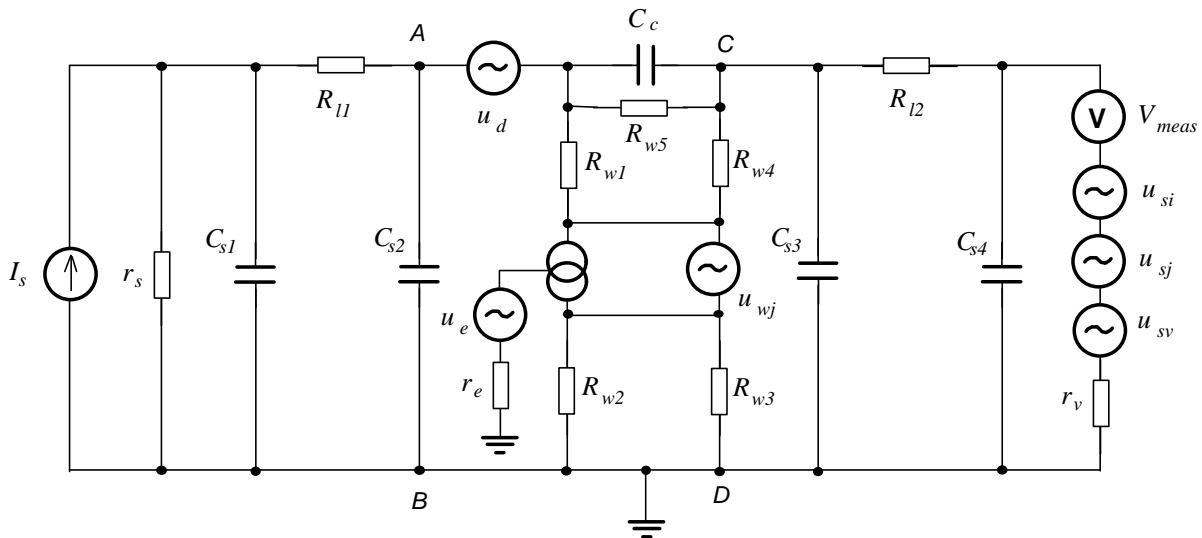
<sup>#</sup> M. Wang's present address: Department of Mine and Mineral Engineering, University of Leeds, LS2 9JT

### 2. NOISE MODEL

To understand noise levels and search optimum methods for acquiring accurate data from physical measurement, a noise model as given in Figure 1 is derived to simulate the electrical measurement properties of a blast furnace. A four-electrode technique has been employed, to obtain boundary voltage measurements from the blast furnace, in which current is injected to one of electrode pairs and voltages are measured from other electrode pairs. From considerations of symmetry only half of the four-terminal measurement system is considered in the model.

#### 2.1 DC excitation and measurement

Electrical properties of an electrically conductive object can normally be obtained using two basic methods – AC or DC excitation and their related measurement methods. The majority of the blast furnace wall is constructed of Carbon. The resistivity of Carbon is given as  $0.0038 \Omega/\text{cm}$  [4] at room temperature. It is well known that the distance that an electromagnetic plane wave can penetrate into a conductor is denoted by  $\delta$  (Equation 1), which is referred to as the depth of penetration or skin depth.



$I_s$ : current source;  
 $r_s$ : output impedance of  $I_s$ ;  
 $u_d$ : dc overpotential at metal-carbon electrode interface;  
 $u_e$ : noises from environment;  
 $r_e$ : output impedance of  $u_e$ ;  
 $u_{si}$ : input offset voltage of OPA;  
 $u_{sj}$ : Johnson's noise of OPA;  
 $u_{sv}$ : voltage noise of OPA;  
 $u_{wj}$ : Johnson's noise of furnace;  
 $V_{meas}$ : voltage measurement;  
 $r_v$ : input impedance of  $V_{meas}$ ;  
 $C_{s\#}$ : stray capacitance of cables;  
 $C_c$ : cross talking capacitance between cables;  
 $R_{l\#}$ : cables' resistance;  
 $R_{w\#}$ : equivalent resistance of furnace wall;

Figure 1: Noise model for measuring mutual resistance from Blast furnace

The electric field intensity at depth  $\delta$  has 36.8% of its value at the surface of the conductor.

$$d = \frac{1}{\sqrt{pms} f} \quad (1)$$

The electrical parameters and  $\delta$ -values for some conductors are given in the following tables.

materials	$\mu_r$	$\mu$ (h/m)	$\sigma$ (S/m)
graphite brick	1	$1.26 \times 10^{-6}$	$2.5 \times 10^4$
copper	1	$1.26 \times 10^{-6}$	$5.8 \times 10^7$
water	1	$1.26 \times 10^{-6}$	0.01

Table 1 : Electrical Properties

materials	60 Hz	1 kHz	10 kHz
graphite brick	0.41	0.1	0.0318
copper	$8.5 \times 10^{-3}$	$2.09 \times 10^{-3}$	$0.66 \times 10^{-3}$
water	649.0	159.0	50.0

Table 2 : Skin Depth (m) at 36.8% Attenuation

Clearly, only a DC approach can give useful information inside a blast furnace due to the skin effect in the highly conductive hearth. Besides the skin effect the bulk resistance of hearth,  $R_{w\#}$ , is also a function of temperature. A nonlinear temperature coefficient gives a value 0.0025  $\Omega\text{cm}$  for the resistivity of Carbon at 1000  $^\circ\text{C}$ . This is about 67% of the resistivity at room temperature. However, weekly temperature excursions of 150  $^\circ\text{C}$  [6] have been reported in

the outer regions of the hearth during operation of the blast furnace. This results in a resistivity change that is about  $\pm 5\%$  of the weekly average value.

## 2.2 Current source $I_s$ and $r_s$

A current source is usually employed to energise the measurement volume for electrical impedance tomography. It wouldn't be difficult to build such a source with a capacity to output large current and reasonably high output impedance. Since the load resistance from the furnace hearth is less than 1  $\text{m}\Omega$ , it is possible to construct the current source using a conventional voltage source together with a resistor for current limitation.

Beside the parameters described above, the other parameters in the noise model that could affect the measurement accuracy are the cable resistance  $R_{l\#}$  and the electrode overpotential  $u_d$ . The effect of other noise sources could be reduced by integrating measurements over a long period, together with some calibration techniques.

## 2.3 Cable resistance $R_{l\#}$

The temperature coefficient,  $d_t$ , of Copper is approximately constant in the range from 0 to 1500 K having a value of about  $6.7 \times 10^{-11}$

$\Omega\text{m}/^\circ\text{C}$ . The resistance of 100 meters cable (RG59) at 273 K is

$$d_t \times 273 \times 100 / (\text{X-sectional area}) = 5.69\Omega \quad (2)$$

For a temperature change of 20 °C from 273 K, the relative resistivity change is

$$(r_{t1} - r_{t0}) / r_{t0} = (293 - 273) / 273 = 7.3\% \quad (3)$$

This gives a resistance change of about 0.42  $\Omega$ . This change would not produce a significant effect on the results from a laboratory-scale model but, in practice, it could result in errors for daily-recorded data. This error can be reduced by integrating over a long period.

### 2.4 DC overpotential, $u_d$ , at metal-carbon electrode interface

A DC potential may be present at the interface of two different metals. The value may be of the order of mV and variable with each electrode interface and operation temperature. This is unlikely to affect the results from a laboratory-scale model. This error can be reduced by employing a switched DC supply and integrating over a long period.

## 3. 'COLD' MODEL AND EXPERIMENT SETUP

A 'cold' model made from graphite blocks (conductivity =  $2.5 \times 10^4$  S/m) has been assembled as a laboratory-scale 'blast furnace' at UMIST. It consists of one graphite 'cup' ( $\phi 47.6\text{cm}$ ), two graphite rings with different diameter ( $\phi 37.4\text{cm}$  and  $\phi 32.2\text{cm}$ ), two graphite disks ( $\phi 37.4\text{cm}$ ) and one steel case ( $\phi 54.6\text{cm}$ ). These rings and disks are used to represent changes of hearth thickness. Twenty-five holes for mounting electrodes are machined in the steel case. Copper electrodes ( $\phi 5.0\text{cm}$ ) are mounted through these holes and then, contact is established with the outside surface of the graphite cup. A conventional ring sensor (16 electrodes) plus a flat sensor in the base of the 'hearth' (9 electrodes) are formed from these electrodes. At the present stage only one graphite cylinder, with diameter 32.2cm, and the ring sensor have been used to obtain tomographic information related to a change of wall thickness in the cold model. To improve contact between the cup and the inner ring, graphite powder has been compressed into the gap between them. The conductivity of the compressed graphite powder has been measured to be  $1.0 \times 10^2$  S/m.

A DC excitation and measurement strategy has been employed for the sixteen-electrode sensing ring. One Ampere current, generated from a

Thurlby PL310 power supply, together with a 4.7  $\Omega$  resistor is applied to one pair of electrodes and boundary voltages are measured from other electrode pairs using a Keithley2001 nanovolt meter. The construction of the cold model with the basic cup and measurement configuration is shown in Figure 2. The cold model with a change of 'hearth thickness' provided by a graphite cylinder and compressed powder is shown in Figure 3.

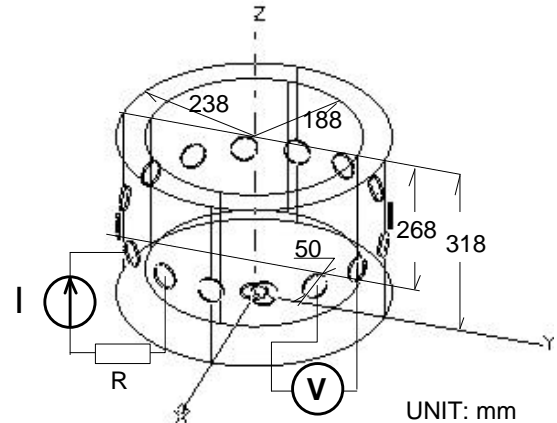


Figure 2: Basic cup in the cold model and its measurement configuration ( $R = 4.7\Omega$ ,  $I = 1\text{A}$ )

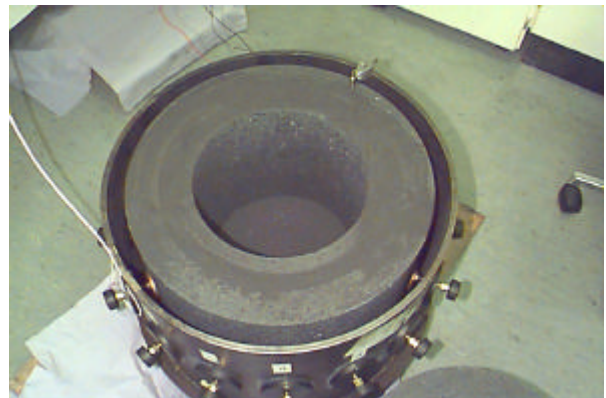


Figure 3: A basic cup conjoined with an inner ring using graphite powder.

## 4. RESULTS FROM MEASUREMENT AND SIMULATION

Measurements have been obtained from the basic cup (Cup) and the cup with the change of wall thickness (CPR) as described in section 3. Considering the axial symmetry in these setups, only one profile is measured for each setup. The raw measurements and their relative changes are given in Figure 4. The maximum change due to adding the inner ring and the compressed graphite powder is of the order of 20% even though the conductivity of the graphite powder is 250 times less than that of the graphite cup and the inner ring.

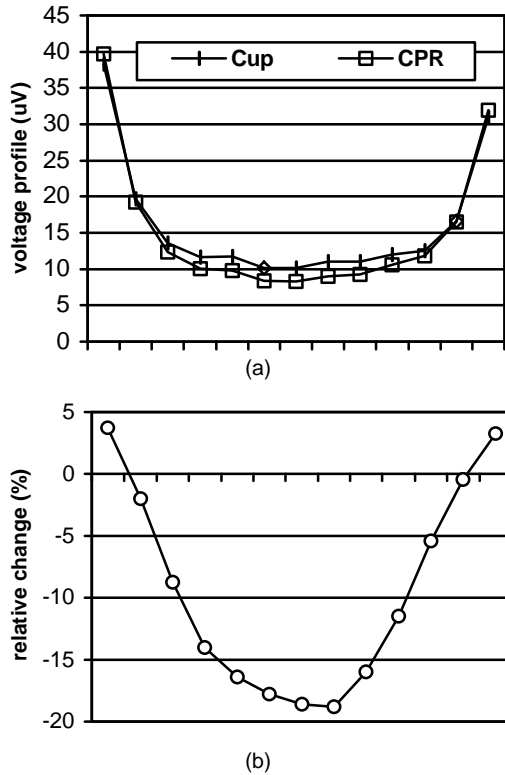


Figure 4: (a) measured voltage profiles and (b) their relative changes using the basic cup (Cup) and the cup conjoined with the inner ring using compressed graphite powder (CPR).

In order to compare results from measurements and also evaluate the results from simulation, a number of three-dimensional models have been simulated based on the exact dimensions and conductivity of the cold model. Boundary voltages have been simulated using the Ansoft Maxwell 3-D electrostatic field simulation package. The conductivity of graphite and powder, in the simulation, is  $2.5 \times 10^4$  S/m and  $1 \times 10^2$  S/m respectively. Figure 5a shows the simulated boundary profiles obtained using a solid graphite cylinder (Sref), a basic graphite cup (SCup) and the cup conjoined with a graphite inner ring using graphite powder (SCPR). Their relative changes are given in Figure 5b.

The profiles obtained from measurement (Figure 4) and simulation (Figure 5), display similar trends and absolute values. The consistency between the results obtained from measurement and simulation, suggests reliability and accuracy in the measurements.

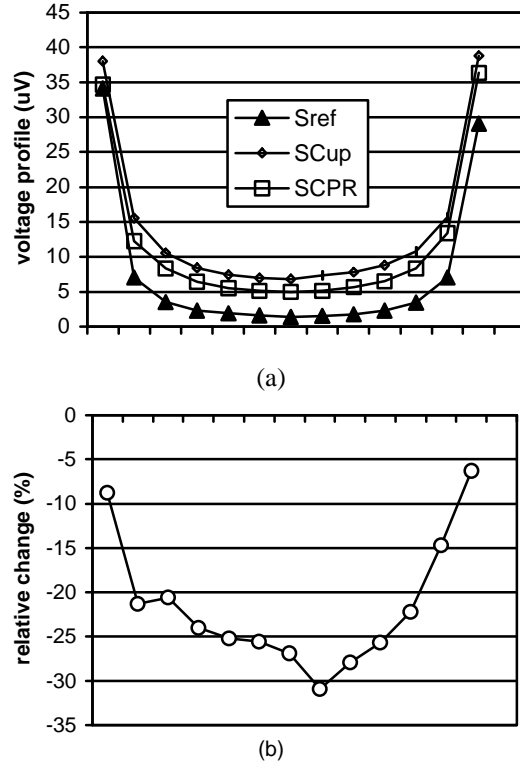


Figure 5: (a) simulated voltage profiles and (b) their relative changes. Basic cup (SCup), Cup with inner ring and compressed graphite powder (SCPR) and solid cylinder (Sref)

Based on the principle of axial symmetry, data errors can be easily found in these boundary voltage profiles obtained from both measurement and 3-D simulation. There is possibly less error in measurement compared to simulation. Therefore, data are further processed by averaging data measured at two symmetrical positions. Similarly, only one profile (13 data points) is measured or simulated and then used to determine a full set of boundary voltages (104 data).

Due to difficulties in obtaining reference boundary voltages from a solid graphite cylinder (we have not got one), a simulated boundary profile (Sref) is also used for imaging the actual conductivity distribution. Comparing the simulated profiles (Figure 5) and measured profiles (Figure 4), this is felt to be acceptable except for a small shift.

The 2-dimension sensitivity theorem method (STM) [5] is used as one method for mapping the changes of conductivity in the cold model. Both the forward and inverse solvers are based on the Conjugate Gradient method (CG) [7]. The final result is found after a number of iterations which is determined from the signal to noise ratio (SNR) of measurement.

$$[\bar{g}] = -[\bar{s}]^T [\bar{s}]^{-1} [\bar{s}]^T [\bar{h}] \quad (4)$$

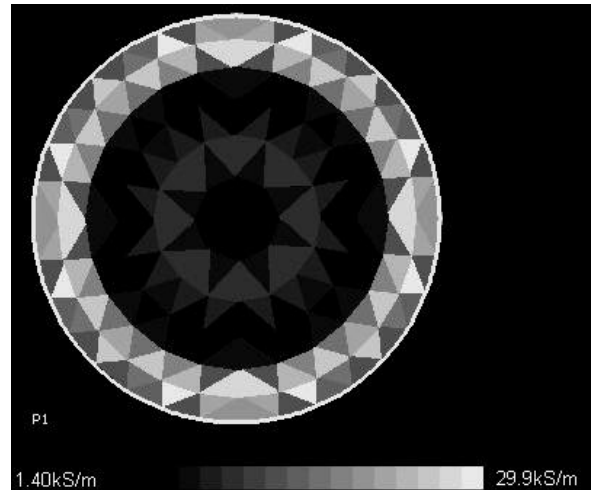
where

$$\bar{h}, \bar{g}, \bar{s}$$

are the normalised changes of boundary measurements, changes of conductivity and the sensitivity matrix respectively.

The conductivity maps of the basic cup are reconstructed as Figures 6a and 6b representing data from measurement and simulation respectively. The profile simulated from the solid graphite block (Sref) is used as a reference for image reconstruction. The reconstructed images show a clear sharp wall. However, the images reconstructed using data obtained from a change of wall thickness do not give a clear difference from the images of the basic cup. This could be due to the sensitivity and limitation of the forward approach to the small difference between these relative changes of boundary profiles.

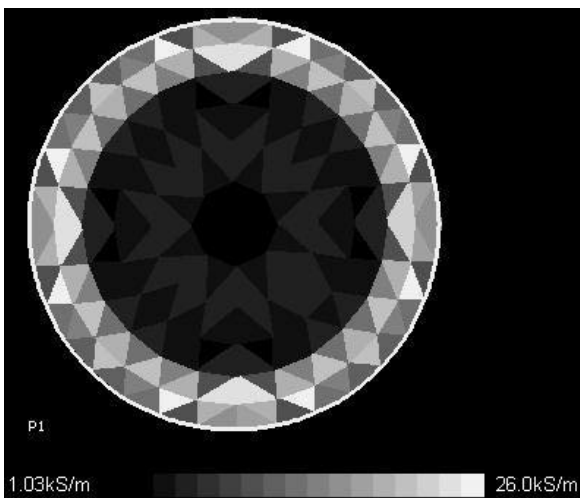
To reveal the small change of conductivity distribution, a differential imaging method has been employed. Instead of using the reference profile obtained from the homogeneous solid graphite cylinder, the differential imaging method uses the profile obtained from the initial conductivity. The conductivity difference between the basic cup and the change of wall thickness has been reconstructed using the differential imaging method. The results are shown in Figure 7a and 7b, which are related to data obtained from measurement and simulation respectively. The profiles obtained from the basic cup are used as a reference for both cases. For these differential images, changes of wall thickness are suggested by the regions of high conductivity which can be seen as bright circles surrounding the central dark region.



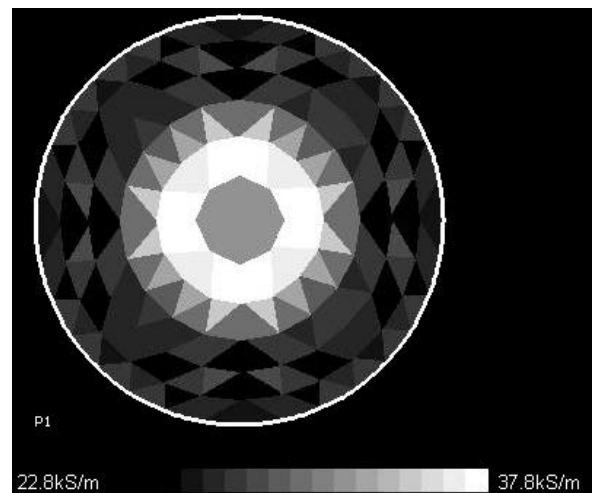
(b)

Figure 6: Reconstructed images of the basic cup using (a) data obtained from measurement and (b) simulation.

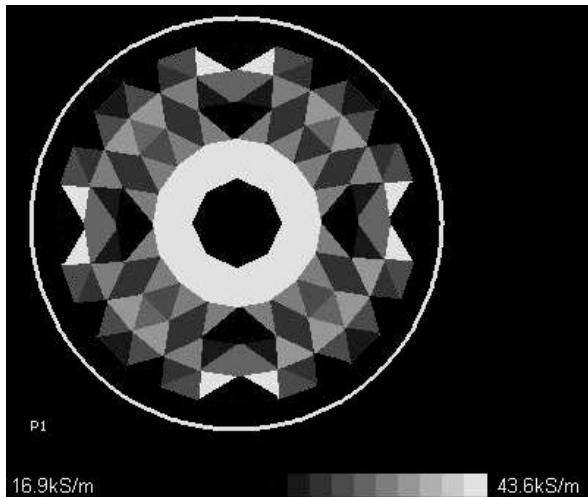
The diameter of the bright circles is less than would be expected from the dimensions of the graphite cylinder, as shown in Figure 3. It is likely that this reduced diameter is due to 3-D effects. The images are reconstructed using a 2-D algorithm that treats all data as if the fields were restricted to a 2-D domain. In reality the field is not constrained and extends above and below the plane of the electrodes. This suggestion has been explored by the use of a 2-D forward solver. Using the conductivity distribution that is predicted by the reconstruction algorithm the 2-D solver calculates boundary voltages that are very close to those that have been measured and this supports the assertion that 3-D effects may be responsible for the discrepancies.



(a)



(a)



(b)

Figure 7: Differential imaging of the small changes of wall thickness. (a) reconstructed with data obtained from measurement, (b) reconstructed with data obtained from simulation.

## 5. DISCUSSION AND CONCLUSIONS

A DC excitation and measurement strategy using a commercial voltage meter and a voltage source has been used for obtaining tomographic measurements from a laboratory-scale 'cold model' of a blast furnace hearth. The static, adjacent electrode, measurements reveal a range from 5.0 to 40  $\mu\text{V}$  for 1A, DC, current injection for the basic cup. A maximum change of -20% is observed due to adding a graphite powder layer and a graphite ring inside the cup. These boundary voltages and their changes have been successfully measured at an accuracy better than 5%.

From the tomographic measurements a conductivity distribution with a sharp boundary between graphite and air has been reconstructed using the STM algorithm. Using the differential imaging method it has been possible to image changes in wall thickness.

Further development of a 3-D reconstruction or 3-D converting algorithm, based on prior-knowledge of a blast furnace, could improve the accuracy of imaging. In practice, the switched DC voltage supply technique together with large current injection and integration over a long period may be able to provide an acceptable level of accuracy for monitoring hearth thickness in a blast furnace.

## REFERENCES

- [1] Leprince, G., Picard, M., Temoin, F. and Libralesso, J.M., "Hearth erosion: measurements and modeling", 2<sup>nd</sup> European Ironmaking Congress, 1993, pp 405-408
- [2] Fujiyosi, S., Inoue, M., Watanabe, H. and Kamiyama, H., "The development of nondestructive measuring on refractories for iron and steel making", Proceeding of 6<sup>th</sup> International Iron and Steel Congress, 1990, pp 215-222
- [3] He, R., Wang, M. and York, T., "Characterization of electrical conductivity of refractory samples supplied by BS", TFC research report - UMA05001, UMIST, Sep.1997.
- [4] Charles, L. M., "Carbon and Graphite Handbook", Interscience Publishers, 1968, p. 34
- [5] Wang, M., Mann, R. and Dickin, F., "Electrical resistance tomographic sensing systems for industrial applications", Chem. Eng. Comm., in press, 1998, p. 1-22
- [6] James, E.T. "A communication letter to He. R", BS file ref. T/2244/98, 20<sup>th</sup> Aug. 1997
- [7] Jennings, A. and McKeown, J.J., "Matrix Computation", John Wiley & Sons Ltd. 1992